

# Time-harmonic torsional waves in a composite cylinder with an imperfect interface

J. R. Berger<sup>a)</sup>

*Division of Engineering, Colorado School of Mines, Golden, Colorado 80401*

P. A. Martin<sup>b)</sup>

*Department of Mathematics, University of Manchester, Manchester M13 9PL, United Kingdom*

S. J. McCaffery<sup>c)</sup>

*Division of Engineering, Colorado School of Mines, Golden, Colorado 80401*

(Received 24 June 1999; accepted for publication 12 November 1999)

In this paper, the propagation of time-harmonic torsional waves in composite elastic cylinders is investigated. An imperfect interface is considered where tractions are continuous across the interface and the displacement jump is proportional to the stress acting on the interface. A frequency equation is derived for the rod and dispersion curves of normalized frequency as a function of normalized wave number for elastic bimetals with varying values for the interface constant  $F$  are presented. The analysis is shown to recover the dispersion curves for a bimaterial rod with a perfect (welded) interface ( $F=0$ ), and has the correct limiting behavior for large  $F$ . It is shown that the modes, at any given frequency, are orthogonal, and it is outlined how the problem of reflection of a torsional mode by a planar defect (such as a circumferential crack) can be treated. © 2000 Acoustical Society of America. [S0001-4966(00)04402-7]

PACS numbers: 43.20.Mv, 43.20.Gp, 43.35.Cg, 43.38.Dv [ANN]

## INTRODUCTION

The motivation for this study comes from the application of electromagnetic–acoustic transducers (EMATs) to the nondestructive testing of reinforced cables. We model the cable as an infinitely long bimaterial cylinder, with a core of circular cross section surrounded by a coaxial cladding; the core and the cladding are different homogeneous isotropic elastic solids.

Applications of EMATs are reviewed by Frost (1979) and by Hirao and Ogi (1997). We are interested in the use of time-harmonic torsional waves in the composite cylinder. Johnson *et al.* (1994) have used EMATs to study standing torsional modes in a single-material circular cylinder. This is a classical problem originally studied by Pochhammer (see, for example, Achenbach, 1973, sec. 6.10, or Miklowitz, 1978, sec. 4.4).

Propagation of time-harmonic torsional waves in a rod composed of two or more elastic layers has also been studied; see Thurston's paper (1978) for a comprehensive review. Perhaps the earliest work is by Armenàkas (1965, 1967, 1971). He studied the dispersion of harmonic waves and established the displacements and stresses at the interface of each layer analytically. A frequency equation was obtained by enforcing continuity conditions at the interface and a stress-free boundary condition on the lateral surfaces of the cylindrical rod.

Charalambopoulos *et al.* (1998) have considered the free

vibration of a bimaterial elastic rod of finite length. The problem was solved for time-harmonic waves using the Helmholtz decomposition of the three-dimensional elasticity equations. The interface between the layers was considered as perfect, providing continuity of displacement and traction. The frequency equation for the full three-dimensional rod was found in terms of a  $9 \times 9$  determinantal equation whose roots yield the dispersion relations for the rod.

Rattanawangcharoen and Shah (1992) have also considered the layered cylindrical rod, but they studied the problem from a more general perspective in that their formulation allowed many layers. A propagator matrix approach was used which related the stresses and displacements of one layer to the next. The propagator matrix was found to implicitly generate the frequency equation for the rod. The main motivation for the paper was to arrive at an efficient computational scheme for the many-layer problem which did not rely on a homogenization method such as integrating through the layers.

In this paper, we consider the bimaterial elastic cylinder with an imperfect interface between the core and the cladding. We do this because it is unrealistic to assume a perfectly bonded (welded) interface for our intended application to reinforced cables. We model the imperfect interface using a (linear) modification to the standard perfect-interface conditions, allowing some slippage. The interface conditions involve a single dimensionless parameter  $F$ . We study the effect of varying  $F$  on the dispersion relations. Note that the results for a perfectly bonded interface can be recovered by setting  $F=0$ .

EMATs can be used to excite propagating modes with a specified axial wavelength  $\lambda$ , where  $\lambda$  is determined by the physical spacing between the magnets of alternating polarity.

<sup>a)</sup>Electronic mail: jberger@mines.edu

<sup>b)</sup>Present address: Department of Mathematical and Computer Sciences, Colorado School of Mines, Golden, CO 80401; electronic mail: pamartin@mines.edu

<sup>c)</sup>Present address: CIRES, University of Colorado, Boulder, CO 80309.

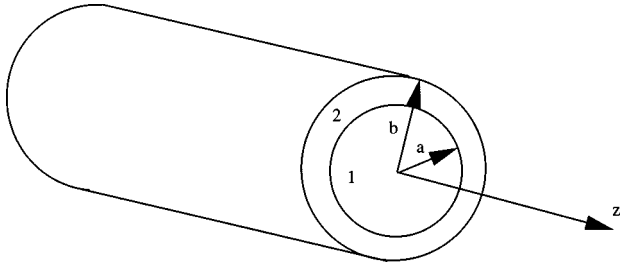


FIG. 1. Geometry of the bimaterial cylinder.

One then adjusts the frequency  $\omega$  until one of the propagating torsional modes is excited. When such a mode interacts with a defect in the composite cylinder, other allowable modes at the frequency  $\omega$ , but with various wavelengths, will be stimulated; evanescent modes (decaying exponentially with distance from the defect) will also be present, in general. We show that the torsional modes at a given frequency are orthogonal, extending a proof due to Gregory (1983). We also discuss the evanescent modes and their computation.

Finally, we outline how our knowledge of the modal structure for the composite cylinder can be used to model the problem of reflection of a torsional mode by a thin defect in a cross-sectional plane. The EMAT system can only receive waves with the same wavelength as the incident mode, so that some information at the excitation frequency  $\omega$  is lost; but the experiment can be repeated at other modal frequencies.

## I. FORMULATION

Let  $(r, \theta, z)$  be cylindrical polar coordinates. We consider the infinite isotropic elastic bimaterial cylinder shown in Fig. 1. The cylinder consists of a solid core,  $r < a$ , surrounded by an annular cladding,  $a < r < b$ ; the core and cladding are made of materials 1 and 2, respectively. Material  $m$  has Lamé moduli  $\lambda_m$  and  $\mu_m$ ,  $m = 1, 2$ . The analysis presented here generally follows Armenakias (1965).

In general, the displacement field  $\mathbf{u} = (u, v, w)$  in each portion of the bimaterial can be written using the Lamé scalar potential  $\phi$  and vector potential  $(\psi_r, \psi_\theta, \psi_z)$ ; see, for example, Achenbach, 1973, sec. 2.13. We are interested in torsional waves, for which the only non zero displacement component is the tangential displacement  $v$ , and  $v$  itself is required to be independent of  $\theta$ . Hence, the only potential needed is the  $z$ -component of the vector potential,  $\psi_z \equiv \psi$ , say. In terms of  $\psi$ , we have

$$v = -\frac{\partial \psi}{\partial r}. \quad (1)$$

The only nontrivial stress components are

$$\sigma_{r\theta} = \mu \left( \frac{\partial v}{\partial r} - \frac{v}{r} \right) \quad (2)$$

and

$$\sigma_{\theta z} = \mu \frac{\partial v}{\partial z}. \quad (3)$$

The potential  $\psi$  satisfies

$$\Delta \psi = \frac{1}{c^2} \frac{\partial^2 \psi}{\partial t^2}, \quad (4)$$

where  $\Delta$  is the Laplace operator and  $c$  is the shear wave speed. For waves propagating in the positive  $z$ -direction, the appropriate solution of (4) can be written as

$$\psi(r, z, t) = \Psi(r) e^{i(kz - \omega t)}, \quad (5)$$

where  $i$  is  $\sqrt{-1}$ ,  $k$  and  $\omega$  are real, and  $\Psi$  solves

$$\frac{1}{r} \frac{d}{dr} (r \Psi') + ((\omega/c)^2 - k^2) \Psi = 0. \quad (6)$$

This is Bessel's equation of order zero. Its solutions depend on the sign of  $\omega^2 - k^2 c^2$ . Thus, define

$$Z_n = J_n, \quad W_n = Y_n, \quad \text{and } q = \sqrt{(\omega/c)^2 - k^2} \quad \text{if } \omega^2 > k^2 c^2, \quad (7)$$

and

$$Z_n = (-1)^n I_n, \quad W_n = K_n, \quad \text{and } q = \sqrt{k^2 - (\omega/c)^2} \quad \text{if } \omega^2 < k^2 c^2, \quad (8)$$

where  $J_n$  and  $Y_n$  are Bessel functions and  $I_n$  and  $K_n$  are modified Bessel functions. The factor  $(-1)^n$  will allow a unified treatment for all frequencies. The behavior of the solution as  $q \rightarrow 0$  will be examined in some detail later; for now we assume that  $q > 0$  ( $\omega^2 \neq k^2 c^2$ ).

So, the appropriate solution of (6) is

$$\Psi(r) = q^{-2} A Z_0(qr) + b^2 B W_0(qr), \quad (9)$$

where  $A$  and  $B$  are arbitrary constants, and the factors  $q^{-2}$  and  $b^2$  have been introduced for later convenience, implying that  $A$  and  $B$  are dimensionless; recall that  $b$  is the outer radius.

The displacement field obtained by substituting (5) and (9) in (1) is

$$v = \{q^{-1} A Z_1(qr) + q b^2 B W_1(qr)\} e^{i(kz - \omega t)}, \quad (10)$$

as  $Z'_0(x) = -Z_1(x)$  and  $W'_0(x) = -W_1(x)$ . (Note that  $I'_0 = I_1$ .) From (2), we obtain for the stress,

$$\sigma_{r\theta} = -\mu \{A Z_2(qr) + (qb)^2 B W_2(qr)\} e^{i(kz - \omega t)}, \quad (11)$$

as  $Z'_1(x) - x^{-1} Z_1(x) = -Z_2(x)$  and  $W'_1(x) - x^{-1} W_1(x) = -W_2(x)$ .

Let us now use the expressions above, using subscripts 1 and 2 to indicate quantities in the core and cladding, respectively. Thus, from (10), the displacement in the cladding is

$$v_2 = \{q_2^{-1} A_2 Z_1(q_2 r) + q_2 b^2 B_2 W_1(q_2 r)\} e^{i(kz - \omega t)}. \quad (12)$$

For the core, the solution for  $v_1$  must be bounded at the origin so we have

$$v_1 = q_1^{-1} A_1 Z_1(q_1 r) e^{i(kz - \omega t)}. \quad (13)$$

In these expressions,  $q_j$  is defined by

$$q_j = \begin{cases} \sqrt{k_j^2 - k^2} & \text{if } k_j^2 > k^2, \\ \sqrt{k^2 - k_j^2} & \text{if } k_j^2 < k^2, \end{cases} \quad j = 1, 2, \quad (14)$$

where  $k_j = \omega/c_j$ . Note that the wave number,  $k$ , is the same in the expressions for  $q_1$  and  $q_2$ ; this observation gives a

relation between  $q_1$  and  $q_2$ , which we will discuss later.

With reference to Fig. 1, we now consider boundary and interface conditions on the displacement field given by (12) and (13). At the outer surface, we have the traction-free boundary condition

$$\sigma_{r\theta}=0 \quad \text{at } r=b. \quad (15)$$

We consider the interface conditions in the following section.

### A. Interface conditions

A variety of conditions may be taken on the interface  $r=a$  in order to represent imperfect interface conditions. A review of interface conditions for elastic wave problems has been presented by Martin (1992). For most models, the displacement  $\mathbf{u}^+$  and traction  $\mathbf{t}^+$  on one side of the interface are assumed to be linearly related to the displacement  $\mathbf{u}^-$  and traction  $\mathbf{t}^-$  on the other side of the interface. For example, the model of Rokhlin and Wang (1991), originally derived for plane interfaces, takes interface conditions of the form

$$[\mathbf{t}] = \mathbf{G}\mathbf{u}^- + \mathbf{B}\mathbf{t}^-, \quad [\mathbf{u}] = \mathbf{F}\mathbf{t}^- + \mathbf{A}\mathbf{u}^-,$$

where  $\mathbf{A}$ ,  $\mathbf{B}$ ,  $\mathbf{F}$ , and  $\mathbf{G}$  are  $3 \times 3$  matrices, and the square brackets indicate a jump in the quantity across the interface; for example, if the interface is at  $r=a$ , we have

$$[\mathbf{u}] = \mathbf{u}^+ - \mathbf{u}^- = \mathbf{u}(a^+, \theta) - \mathbf{u}(a^-, \theta), \quad (16)$$

suppressing the dependence on  $z$  and  $t$ . If the coupling term  $\mathbf{G}$  can be neglected, and furthermore if  $\mathbf{A}$  and  $\mathbf{B}$  are set equal to zero, we recover the model of Jones and Whittier (1967) for a flexibly bonded interface,

$$[\mathbf{t}] = 0, \quad (17)$$

$$[\mathbf{u}] = \mathbf{F}\mathbf{t}^-, \quad (18)$$

where  $\mathbf{F}$  is a constant diagonal matrix. For simplicity, we will use the Jones–Whittier model for the analysis presented here. For thin, elastic interfacial layers, the elements of  $\mathbf{F}$  have been related to the thickness and elastic constants of the layer by, for example, Jones and Whittier (1967), Mal and Xu (1989), and Pilarski and Rose (1988).

For torsional waves,  $\mathbf{u}$  reduces to a scalar for the tangential displacement  $v$  and  $\mathbf{t}$  reduces to a scalar for the tangential shear stress  $\sigma_{r\theta}$ . The interface conditions are then

$$\sigma_{r\theta}(a^-) = \sigma_{r\theta}(a^+) \quad (19)$$

and

$$[v] = (a/\mu_1)F\sigma_{r\theta}(a), \quad (20)$$

where  $[v] = v_2(a^+) - v_1(a^-)$  and  $F$  is a dimensionless scalar. Our goal is to investigate solutions which satisfy (15), (19), and (20) as the interface parameter  $F$  is varied. We note that if  $F=0$ , the perfect interface conditions of continuity of traction and displacement are recovered.

## II. FREQUENCY EQUATION FOR THE ROD

We now present the details for the set of equations which will determine the dispersion relations in the bimaterial rod. Substituting the displacement field of (12) in the boundary condition, (15), yields

$$A_2 Z_2(q_2 b) + (q_2 b)^2 B_2 W_2(q_2 b) = 0. \quad (21)$$

Following the Jones–Whittier model, we have for continuity of traction across the interface, from (12), (13), and (19),

$$(\mu_1/\mu_2)A_1 Z_2(q_1 a) - A_2 Z_2(q_2 a) - (q_2 b)^2 B_2 W_2(q_2 a) = 0. \quad (22)$$

Note that neither of these equations changes in the case of the perfectly bonded interface. The displacement jump across the interface is given by (20). We then have

$$(q_1 b)^{-1} A_1 \{Z_1(q_1 a) - F q_1 a Z_2(q_1 a)\} - (q_2 b)^{-1} A_2 Z_1(q_2 a) - q_2 b B_2 W_1(q_2 a) = 0. \quad (23)$$

Equations (21)–(23) provide three equations in the three unknown constants  $A_1$ ,  $A_2$ , and  $B_2$ . In matrix form, the system of equations is

$$\mathbf{D}\mathbf{b} = \mathbf{0}, \quad (24)$$

where the elements of the nonsymmetric matrix  $\mathbf{D}$  are obtained directly from (21)–(23) and  $\mathbf{b} = (A_1, A_2, B_2)^T$ .

For a nontrivial solution we then require

$$\det \mathbf{D} = 0. \quad (25)$$

This is the frequency equation for the rod.

The quantity  $\det \mathbf{D}$  seems to depend on only five dimensionless parameters, namely

$$q_1 b, \quad q_2 b, \quad a/b, \quad \mu_1/\mu_2, \quad \text{and } F; \quad (26)$$

in particular, the density ratio (or, equivalently,  $c_1/c_2$ ) does not appear explicitly. However, this is illusory: we have to know how to choose  $Z_n$  ( $J_n$  or  $(-1)^n I_n$ ?) and  $W_n$  ( $Y_n$  or  $K_n$ ?) in each material, and these choices depend on the relative sizes of  $k^2$ ,  $k_1^2$ , and  $k_2^2$ , information that we cannot extract from a knowledge of (26) alone.

Thus we proceed as follows. Assume that we are given values for  $a/b$ ,  $\mu_1/\mu_2$ ,  $F$ , and

$$c_2/c_1 = k_1/k_2 = \alpha, \quad (27)$$

say. Choose a value for the axial wave number  $kb$ . We now seek values of  $k_2 b$ , say, so that (25) is satisfied. Note that  $k_1 b = \alpha k_2 b$ , and then  $q_1 b$  and  $q_2 b$  are defined by (14), with the associated selections of  $Z_n$  and  $W_n$  dictated by (7) and (8). In fact, the relations between  $q_1$ ,  $q_2$ ,  $k_1$ ,  $k_2$ ,  $k$ , and  $\alpha$  are complicated, because they depend on the relative magnitudes of  $k^2$ ,  $k_1^2$ , and  $k_2^2$ ; there are four cases, as summarized in Table I. In this table, the second column specifies the four cases in terms of the shear wave speeds of the two materials (these are material constants) and the axial wave speed  $c_a = \omega/k$ . A similar table was given by Kleczewski and Parnes (1987) in their study of torsional modes when the cladding is unbounded ( $b \rightarrow \infty$  in our notation).

In order to compare with Armenakás (1965) (for  $F=0$ ), we have determined the dispersion curves of normalized frequency,

TABLE I. Relations between  $q_1$  and  $q_2$ , in which  $\alpha=c_2/c_1=k_1/k_2$  and  $c_a=\omega/k$ .

Wave numbers	Wave speeds	$q_1^2$	$q_2^2$	Relation between $q_1$ and $q_2$
$k^2 < k_1^2 \leq k_2^2$	$c_1 \leq c_2 < c_a$	$k_1^2 - k^2$	$k_2^2 - k^2$	$q_1^2 = \alpha^2 q_2^2 - k^2(1 - \alpha^2)$
$k^2 < k_2^2 \leq k_1^2$	$c_2 \leq c_1 < c_a$			
$k_2^2 < k^2 < k_1^2$	$c_1 < c_a < c_2$	$k_1^2 - k^2$	$k^2 - k_2^2$	$q_1^2 = -\alpha^2 q_2^2 - k^2(1 - \alpha^2)$
$k_1^2 < k^2 < k_2^2$	$c_2 < c_a < c_1$	$k^2 - k_1^2$	$k_2^2 - k^2$	$q_1^2 = -\alpha^2 q_2^2 + k^2(1 - \alpha^2)$
$k_1^2 \leq k_2^2 < k^2$	$c_a < c_1 \leq c_2$	$k^2 - k_1^2$	$k^2 - k_2^2$	$q_1^2 = \alpha^2 q_2^2 + k^2(1 - \alpha^2)$
$k_2^2 \leq k_1^2 < k^2$	$c_a < c_2 \leq c_1$			

$$\Omega_2 = k_2(b-a)/\pi = \omega(b-a)/(\pi c_2),$$

as a function of normalized axial wave number,

$$\xi = k(b-a)/\pi,$$

for a given value of the interface parameter  $F$ . We note that the frequency equation determined here cannot be written in terms of a single argument such as  $qa$ , which can be done in the case of a rod made from a single material. As such, we study numerical solutions to (25) in the next section for values of  $a/b$ ,  $F$ , and the elastic constants.

### III. DISPERSION CURVES WITH VARYING INTERFACE CONDITIONS

To benchmark the analysis presented here, we first present results which can be directly compared with Armenàkas (1965) in the case of a perfect interface,  $F=0$ . We take  $a/b=0.25$ ,  $\mu_1/\mu_2=10$ , and  $c_1/c_2=1.83$  (so that the density ratio,  $\rho_1/\rho_2=3$ ). We show the dispersion curves of frequency,  $\Omega_2$ , versus wave number,  $\xi$ , for  $F=0$ ,  $F=1$ ,  $F=10$ , and  $F=100$  for the second mode in Fig. 2 and the third

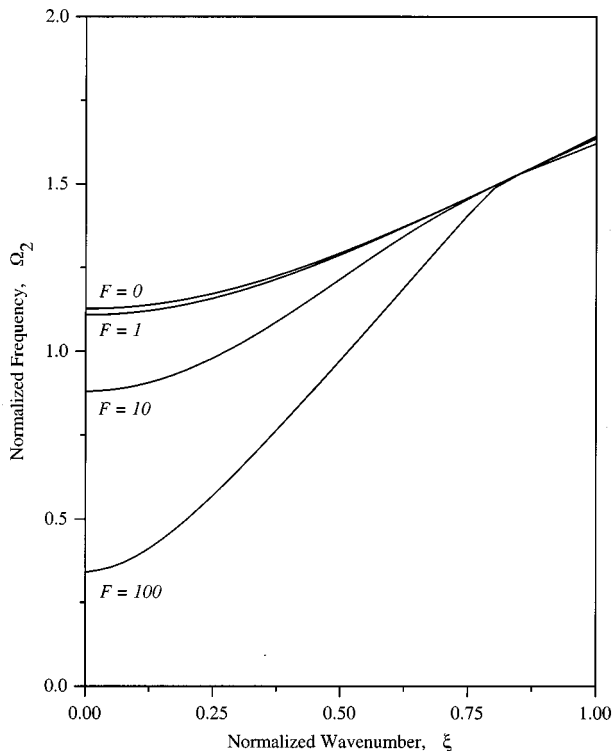


FIG. 2. Dispersion curves for the second mode in the bimaterial cylinder.

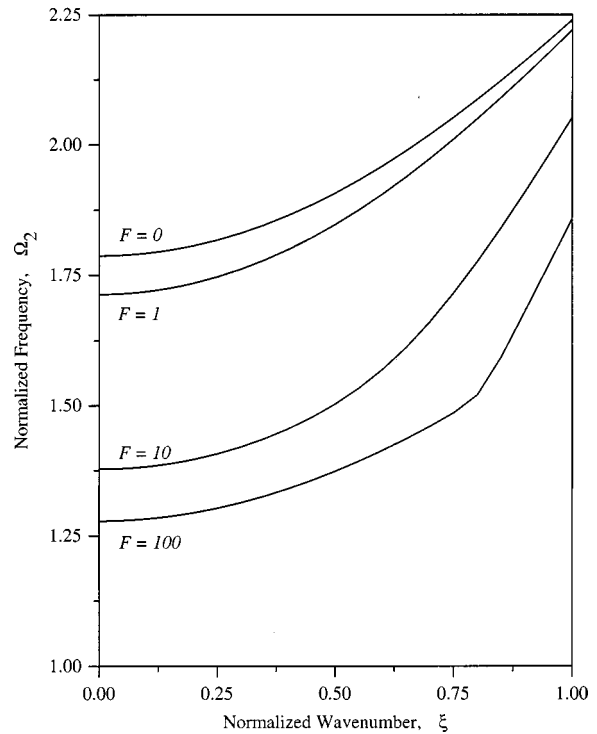


FIG. 3. Dispersion curves for the third mode in the bimaterial cylinder.

mode in Fig. 3. The first mode will be analyzed in a subsequent section. The dispersion curve for  $F=0$  agrees exactly with the analysis of Armenàkas (1965). As the interface parameter is increased, note the decrease in  $\Omega_2$ , especially at the smaller values of  $\xi$ . At higher values of  $\xi$ , the loss of perfect continuity at the interface has a reduced effect.

One feature of note in Fig. 3 is the curve for  $F=100$ , which exhibits a corner at  $\xi \approx 0.8$ . This is not a numerical artifact: the figure was produced using very small increments in  $\xi$ . Similar behavior was found for other (large) values of  $F$ .

A second way of visualizing the behavior of the dispersion curves as the interface parameter is varied is illustrated in Fig. 4. In the figure, we show results for the second mode and plot frequency,  $\Omega_2$ , versus the interface parameter,  $F$ , as the wave number  $\xi$  is varied. As expected, we see a much greater effect on  $\Omega_2$  by  $F$  at the smaller wave numbers. This suggests a possible measurement approach for determining  $F$  where  $\xi$  is fixed,  $\Omega_2$  is measured, and then  $F$  is determined from the figure.

The curves shown in Fig. 4 appear to be approaching asymptotic values for large  $F$ . With reference to the interface conditions given by (20), we see that in the limit as  $F \rightarrow \infty$  we recover the boundary condition

$$\sigma_{r\theta}(a) = 0.$$

This is the appropriate boundary condition for the outer boundary of a solid rod of radius  $a$  and for the inner boundary condition for a hollow tube with inner radius  $a$ . In the case of  $F \rightarrow \infty$ , the frequency equation given by (25) reflects this change in boundary condition,

$$Z_2(q_1 a)g(q_2 a, q_2 b) = 0, \quad (28)$$

where

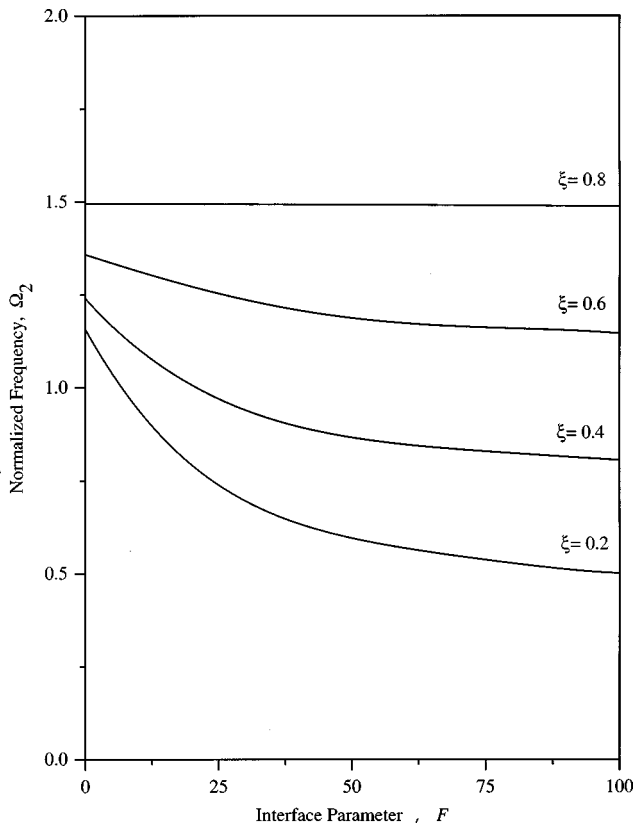


FIG. 4. Normalized frequency vs interface parameter at fixed wave number in the bimaterial cylinder for the second mode.

$$g(q_2a, q_2b) = Z_2(q_2a)W_2(q_2b) - Z_2(q_2b)W_2(q_2a).$$

The frequency equation (28) has two sets of solutions, one given by  $Z_2(q_1a) = 0$  and the other given by  $g(q_2a, q_2b) = 0$ . The first of these is the frequency equation for a solid rod of radius  $a$ , whereas the second is the frequency equation for a hollow tube of inner radius  $a$  and outer radius  $b$ . So, the imperfect interface formulation has the expected behavior for large values of  $F$ .

Numerically, one must be somewhat careful in handling the limit as  $F \rightarrow \infty$  and check if the relations between  $q_1$  and  $q_2$  given in Table I still hold. We present some typical results in Table II where we have used  $F = 1 \times 10^{10}$ . Note in the table that we report values of normalized frequency  $\Omega_2$  as we have throughout this paper, even for the solid rod modes in material 1 reported in the table. From the table, we see that the asymptotic values of frequency,  $\Omega_2$ , for the second mode in the composite rod, are the nondispersive first modes ( $q_1a = 0$ ) in the solid rod. Also, the asymptotic values of

TABLE II. Frequencies for the second and third modes in the composite rod with  $F = 1 \times 10^{10}$ , and corresponding frequencies for the first mode in a solid rod and the second mode in a hollow tube.

$\xi$	$\Omega_2$ second mode	$\Omega_2$ third mode	$\Omega_2$ , hollow tube second mode	$\Omega_2$ , solid rod first mode
0.2	0.365	1.286	1.286	0.365
0.4	0.730	1.332	1.332	0.730
0.6	1.095	1.405	1.405	1.095

frequency,  $\Omega_2$ , for the third mode in the composite rod correspond to the second mode frequencies in the hollow tube.

Some discussion on the interface parameter  $F$  is perhaps in order. As mentioned in the Introduction, the application motivating the analysis presented here is the nondestructive evaluation of reinforced cables. Typically these cables are fabricated with a steel core surrounded by an aluminum cladding. Because of the underlying wire-rope structure of the core and the cladding, the interface conditions are imperfect. Our approach here is to treat the interface parameter in a phenomenological manner to account for the imperfect interface. As such, we do not stipulate a strict physical interpretation to the numerical value of  $F$ , nor do we attempt to relate the value of  $F$  to elastic constants.

#### IV. FIRST TORSIONAL MODE

Armenàkas (1965) noted that the first torsional mode is not properly described by the solution of the Bessel equation, unlike the higher torsional modes analyzed above. Therefore, special consideration of the first torsional mode is necessary, and this is carried out next. For example, when  $q_2 = 0$ , there can be a nondispersive mode propagating in the cladding of the rod with dispersive modes in the core.

Suppose that  $\omega^2 = k^2c^2$ , so that  $q = 0$  and (6) reduces to

$$\frac{d}{dr}(r\Psi') = 0,$$

with general solution

$$\Psi(r) = A + B \log r.$$

This gives a solution for  $v$  proportional to  $B/r$ , which cannot be the general solution as it involves only one arbitrary constant,  $B$ . As we are interested in  $\Psi'$  rather than  $\Psi$ , we return to (6); differentiation with respect to  $r$  gives

$$\frac{d}{dr} \left( \frac{1}{r} \frac{d}{dr} (r\Psi') \right) + ((\omega/c)^2 - k^2)\Psi' = 0,$$

a second-order ordinary differential equation for  $\Psi'$ . When  $\omega^2 = k^2c^2$ , the general solution of this equation is

$$\Psi'(r) = Ar + B/r.$$

Hence, in dimensionless form, we have

$$v(r, z, t) = (Ar + Bb^2/r)e^{i(kz - \omega t)} \quad (29)$$

and

$$\sigma_{r\theta}(r, z, t) = -2\mu B(b/r)^2 e^{i(kz - \omega t)}. \quad (30)$$

Note that the expressions (29) and (30) can also be obtained by taking the limit  $q \rightarrow 0$  in (10) and (11) (apart from some numerical factors which can be absorbed into  $A$  and  $B$ ). This accounts for the various  $q$ -factors in (10): they lead to meaningful (bounded) expressions for small  $q$ .

Let us assume that  $q_2 = 0$ . The outer boundary condition (15) implies that  $B_2 = 0$ , whence  $\sigma_{r\theta} \equiv 0$  in the cladding and

$$v_2 = A_2 r e^{i(kz - \omega t)}. \quad (31)$$

Within the core,  $v_1$  is given by (13). For continuity of tractions across  $r = a$ , (19) gives

$$A_1 Z_2(q_1 a) = 0, \quad (32)$$

whereas the imperfect-interface condition (20) gives

$$A_1 Z_1(q_1 a) - q_1 a A_2 = 0. \quad (33)$$

Now, for nontrivial solutions, we require  $k^2 > k_1^2$ , so that (32) gives  $q_1 a = j_{2,s}$ , the  $s$ -th zero of  $J_2(x)$ . Then  $A_1$  is arbitrary with  $A_2$  given by (33) (with  $Z_1 = J_1$ ). It is interesting to note that the interface parameter  $F$  does not enter into any of the equations, so that the dispersion curves for the first torsional mode when  $q_2 = 0$  are identical, regardless of whether the interface is perfect or imperfect. This is consistent with the fact that since  $q_2 = 0$ , a nondispersive mode is propagating in the cladding and (32) is simply the frequency equation for the dispersive modes in the core.

Alternatively, let us assume that  $q_1 = 0$ ; for bounded displacements in the core, we obtain

$$v_1(r, z, t) = A_1 r e^{i(kz - \omega t)}.$$

Within the cladding,  $v_2$  is given by (12), so that the outer boundary condition gives (21). The interface condition (19) gives

$$A_2 Z_2(q_2 a) + (q_2 b)^2 B_2 W_2(q_2 a) = 0;$$

the frequency equation is then obtained by combining this equation with (21): it is the same equation as for a hollow cylindrical tube. The other interface condition, (20), then determines  $A_1$  as

$$A_1 = (q_2 a)^{-1} A_2 Z_1(q_2 a) + (q_2 b^2/a) B_2 W_1(q_2 a).$$

Again, these equations do not involve  $F$ .

## V. EVANESCENT MODES

So far, we have only considered propagating torsional modes. However, cylinders can also support evanescent modes, which decay exponentially with  $z$ . Such modes can be constructed by writing

$$\psi(r, z, t) = \Psi(r) e^{-kz - i\omega t},$$

where  $\Psi$  solves

$$\frac{1}{r} \frac{d}{dr} (r \Psi') + ((\omega/c)^2 + k^2) \Psi = 0,$$

whence

$$\Psi(r) = q^{-2} A J_0(qr) + b^2 B Y_0(qr)$$

with  $q = \sqrt{(\omega/c)^2 + k^2}$ . Then, proceeding exactly as before, we arrive at the frequency equation (25) in which  $Z_n$  and  $W_n$  are to be replaced by  $J_n$  and  $Y_n$ , respectively.

## VI. DISCUSSION ON MODE ORTHOGONALITY

We have constructed various torsional modes for the composite cylinder in the general form

$$\mathbf{u}(r, \theta, z, t) = \text{Re}\{\mathbf{U}(r, \theta) e^{i(kz - \omega t)}\}.$$

In our computations, we have fixed the axial wave number  $k$  and then calculated the frequencies  $\omega$  of the allowable modes. This is convenient for comparisons with Armenákas (1965) and it is appropriate for the application to EMATs;

these can be used to excite propagating modes of a specified axial wavelength. However, once such a mode has been excited, we are interested in studying its reflection by defects in the cylinder. This is most conveniently done by specifying the frequency and then determining all the allowable modes at that frequency. With this in mind, we write a typical mode as

$$\mathbf{u}^{(n)}(r, \theta, z, t) = \text{Re}\{\mathbf{U}^{(n)}(r, \theta) e^{i(k^{(n)}z - \omega t)}\},$$

where the wave number  $k^{(n)}$  need not be real.

These modes are biorthogonal. To be more explicit, denote the stresses corresponding to  $\mathbf{u}^{(n)}$  by

$$\boldsymbol{\sigma}^{(n)}(r, \theta, z, t) = \text{Re}\{\mathbf{S}^{(n)}(r, \theta) e^{i(k^{(n)}z - \omega t)}\}.$$

Then, if  $k^{(n)} \neq \pm k^{(m)}$ , we have

$$\int_{\mathcal{A}} \{U_z^{(m)} S_{zz}^{(n)} - S_{rz}^{(m)} U_r^{(n)} - S_{\theta z}^{(m)} U_\theta^{(n)}\} r dr d\theta = 0, \quad (34)$$

where  $\mathcal{A}$  is the cross section of the composite cylinder. This relation can be proved by a simple extension of the proof given by Gregory (1983). (One applies the elastic reciprocal theorem twice, once in the core and once in the cladding, and then adds the results; the interface conditions imply that the contributions from integrating over the two sides of the interface cancel.) In fact, (34) holds for all modes in composite cylinders of any cross section, and with any number of imperfect (cylindrical) interfaces. For our problem, with torsional modes given by

$$v^{(n)}(r, z, t) = \text{Re}\{V^{(n)}(r) e^{i(k^{(n)}z - \omega t)}\},$$

Eq. (34) reduces to

$$\int_0^b V^{(m)}(r) V^{(n)}(r) r dr = 0, \quad m \neq n, \quad (35)$$

so that torsional modes are actually orthogonal. This orthogonality relation is useful when the reflection of a torsional mode by certain defects is examined. For example, we may consider a bimaterial cylinder with a planar break (crack) perpendicular to the cylinder's axis, giving an idealized model of a damaged cable. Specifically, we partition the cross-section  $\mathcal{A}$  into a broken part  $\mathcal{A}_b$  and an unbroken part  $\mathcal{A}_u$ , so that  $\mathcal{A} = \mathcal{A}_b \cup \mathcal{A}_u$ . The boundaries of  $\mathcal{A}_b$  and  $\mathcal{A}_u$  are concentric circles; for example, we might take  $\mathcal{A}_u$  to be the circle  $0 \leq r < c$ , with  $\mathcal{A}_b$  as the annulus  $c < r < b$ , so that the cable is circumferentially cracked. Then, if a torsional mode is incident on the defect, the reflected and transmitted fields can be written as modal sums. This is a standard approach for planar obstacles in waveguides. In the context of torsional waves, it has been used recently by Engan (1998) to analyze the effect of a step-change in radius of homogeneous circular cylinders. For the present problem, application of the boundary conditions at the defect plane leads to a system of equations for the reflection and transmission coefficients; of particular interest are the reflected and transmitted modes with the same wavelength as the incident mode, because these are the only modes that can be detected by the EMAT. Again, in a standard way, one can derive integral equations and/or variational expressions for the reflection and transmis-

sion coefficients; see, for example, Schwinger and Saxon (1968) for a detailed discussion on related scattering problems.

## VII. CONCLUSIONS

We have presented an analysis for torsional waves propagating in a bimaterial rod with imperfect interface conditions. To the authors' knowledge, the effect of imperfect interface conditions on dispersive wave motion has not been studied for rods. We find the expected behavior for waves in the rod when we take the interface parameter  $F=0$  and  $F \rightarrow \infty$ . When  $F \neq 0$  we find that the frequency decreases with increasing  $F$  at a given wave number in the dispersion relations. This effect was shown to be more pronounced at small wave numbers. The propagation of nondispersive modes in the cladding was also investigated, and the frequency equation for dispersive modes in the core was recovered. We also showed that, at any given frequency, the modes are orthogonal. This fact can be exploited in the solution of a scattering problem, where an incident torsional mode interacts with an annular defect in the bimaterial rod. The model developed here should be useful in analyzing nondestructive evaluation measurements in reinforced cables where perfect interface conditions may not exist.

## ACKNOWLEDGMENTS

Two of us (J.R.B. and S.J.M.) gratefully acknowledge the support received from the Center for Advanced Control of Energy and Power Systems, a National Science Foundation Industry/University Cooperative Research Center, at the Colorado School of Mines. J.R.B. also acknowledges the additional support provided by the Engineering and Physical Sciences Research Council as a visiting fellow in the Department of Mathematics at the University of Manchester.

Achenbach, J. D. (1973). *Wave Propagation in Elastic Solids* (North-Holland, New York).

- Armenàkas, A. E. (1965). "Torsional waves in composite rods," *J. Acoust. Soc. Am.* **38**, 439–446.
- Armenàkas, A. E. (1967). "Propagation of harmonic waves in composite circular cylindrical shells. I: Theoretical investigation," *AIAA J.* **5**, 740–744.
- Armenàkas, A. E. (1971). "Propagation of harmonic waves in composite circular cylindrical shells. Part II: Numerical analysis," *AIAA J.* **9**, 599–605.
- Charalambopoulos, A., Fotiadis, D. I., and Massalas, C. V. (1998). "Free vibrations of a double layered elastic isotropic cylindrical rod," *Int. J. Eng. Sci.* **36**, 711–731.
- Engan, H. E. (1998). "Torsional wave scattering from a diameter step in a rod," *J. Acoust. Soc. Am.* **104**, 2015–2024.
- Frost, H. M. (1979). "Electromagnetic-ultrasound transducers: Principles, practice, and applications," in *Physical Acoustics*, edited by W. P. Mason and R. N. Thurston (Academic, New York), Vol. 14, pp. 179–275.
- Gregory, R. D. (1983). "A note on bi-orthogonality relations for elastic cylinders of general cross section," *J. Elast.* **13**, 351–355.
- Hirao, M., and Ogi, H. (1997). "Electromagnetic acoustic resonance and materials characterization," *Ultrasonics* **35**, 413–421.
- Johnson, W., Auld, B. A., and Alers, G. A. (1994). "Spectroscopy of resonant torsional modes in cylindrical rods using electromagnetic-acoustic transduction," *J. Acoust. Soc. Am.* **95**, 1413–1418.
- Jones, J. P., and Whittier, J. S. (1967). "Waves at a flexibly bonded interface," *J. Appl. Mech.* **34**, 905–909.
- Kleczewski, D., and Parnes, R. (1987). "Torsional dispersion relations in a radially dual elastic medium," *J. Acoust. Soc. Am.* **81**, 30–36.
- Mal, A. K., and Xu, P. C. (1989). "Elastic waves in layered media with interface features," in *Elastic Wave Propagation*, edited by M. F. McCarthy and M. A. Hayes (North-Holland, Amsterdam), pp. 67–73.
- Martin, P. A. (1992). "Boundary integral equations for the scattering of elastic waves by elastic inclusions with thin interface layers," *J. Nondestruct. Eval.* **11**, 167–174.
- Miklowitz, J. (1978). *The Theory of Elastic Waves and Waveguides* (North-Holland, Amsterdam).
- Pilarski, A., and Rose, J. L. (1988). "A transverse-wave ultrasonic oblique-incidence technique for interfacial weakness detection in adhesive bonds," *J. Appl. Phys.* **63**, 300–307.
- Rattanawangcharoen, N., and Shah, A. H. (1992). "Guided waves in laminated isotropic circular cylinder," *Comput. Mech.* **10**, 97–105.
- Rokhlin, S. I., and Wang, Y. J. (1991). "Analysis of boundary conditions for elastic wave interaction with an interface between two solids," *J. Acoust. Soc. Am.* **89**, 503–515.
- Schwinger, J., and Saxon, D. S. (1968). *Discontinuities in Waveguides* (Gordon & Breach, New York).
- Thurston, R. N. (1978). "Elastic waves in rods and clad rods," *J. Acoust. Soc. Am.* **64**, 1–37.